Physics Letters B 799 (2019) 135035

Contents lists available at ScienceDirect

Physics Letters B

www.elsevier.com/locate/physletb

Neutron spin structure from polarized deuteron DIS with proton tagging

W. Cosyn [a,*], C. Weiss [b]

[a] Department of Physics and Astronomy, Ghent University, Proeftuinstraat 86, B9000 Ghent, Belgium
[b] Theory Center, Jefferson Lab, Newport News, VA 23606, USA

ARTICLE INFO

Article history:
Received 26 July 2019
Received in revised form 22 September 2019
Accepted 17 October 2019
Available online 22 October 2019
Editor: W. Haxton

Keywords:
Polarized deep-inelastic scattering
Neutron
Nuclear fragmentation
Electron-ion collider
Light-front quantization

ABSTRACT

Polarized electron-deuteron deep-inelastic scattering (DIS) with detection of the spectator proton ("tagged DIS") enables measurements of neutron spin structure with maximal control of nuclear effects. We calculate the longitudinal spin asymmetries in polarized tagged DIS using methods of light-front nuclear structure and study their dependence on the measured proton momentum. Asymmetries can be formed with all three deuteron spin states ($\pm 1, 0$) or the two maximum-spin states only (± 1, involving tensor polarization). The proton momentum dependence can be used to select pure S-wave configurations in the deuteron and eliminate D-wave depolarization (transverse momenta $p_{pT} \lesssim 100$ MeV). Free neutron spin structure can be extracted model-independently through pole extrapolation of the tagged asymmetries. Such measurements could be performed at a future electron-ion collider (EIC) with polarized deuteron beams and forward proton detectors.

1. Introduction

Nucleon spin structure studies require measurements of polarized deep-inelastic lepton scattering (DIS) on both the proton and the neutron; see Refs. [1–3] for a review. Proton and neutron data together are needed to determine the flavor composition of the quark helicity distributions, to separate singlet and non-singlet structures in the analysis of scale dependence (QCD evolution, higher-twist effects), and to evaluate the Bjorken sum rule. The neutron spin structure functions are extracted from DIS measurements on polarized light nuclei (deuteron $^2\mathrm{H} \equiv D$, ^{3}He). The procedure must account for nuclear effects such as nucleon spin depolarization, motion of the bound nucleons, non-nucleonic degrees of freedom (e.g. Δ isobars in ^{3}He), and nuclear shadowing and antishadowing [4–11]. The theoretical treatment of these effects is complicated by the fact that they depend strongly on the nuclear configurations present during the high-energy process. In inclusive DIS measurements one accounts for the effects by modeling them in all possible configurations and summing over them, which results in a significant theoretical uncertainty. In view of the experimental precision achievable with a future electron-ion collider (EIC) [12,13], it is necessary to consider new types of measurements that reduce the theoretical uncertainty in neutron spin structure extraction.

DIS on the deuteron with detection of a proton in the nuclear fragmentation region ("tagged DIS"), $e + D \to e' + X + p$, represents a unique method for neutron structure measurements. The deuteron wave function in nucleonic degrees of freedom (pn) is simple and known well up to momenta $\sim$ 300 MeV; Δ isobars are suppressed in the isospin-0 system [14]. The detection of the proton identifies events with active neutron and eliminates dilution. The measurement of the proton momentum fixes the nuclear configuration during the high-energy process and enables a differential treatment of nuclear effects. Extrapolation of the measured proton momentum dependence to the on-shell point eliminates nuclear initial-state modifications and final-state interactions and permits the extraction of free neutron structure [15]. In tagged DIS in fixed-target experiments, the proton emerges with typical momenta $|\boldsymbol{p}_p| \lesssim 100$ MeV and is captured with special detectors placed close to the target (JLab 6/12 GeV BONuS [16–18], ALERT [19]). In collider experiments at EIC, the proton moves forward with $\sim 1/2$ the deuteron beam momentum and is detected with forward detectors integrated in the interaction region and beam optics. The collider setup offers many advantages for tagging (no target material, acceptance at proton rest-frame momenta $|\boldsymbol{p}_p| \sim 0$, good momentum resolution), and the physics potential was stud-

* Corresponding author.
E-mail addresses: wim.cosyn@ugent.be (W. Cosyn), weiss@jlab.org (C. Weiss).

https://doi.org/10.1016/j.physletb.2019.135035

ied in an R&D project [20,21]. With the possibility of polarized deuteron beams at EIC, it is interesting to assess the potential of polarized tagged DIS for precise measurements of neutron spin structure.

In this letter we report about the development of a theoretical framework for neutron spin structure measurements with polarized tagged DIS in collider experiments; see Ref. [22] for an earlier study. Using methods of light-front (LF) nuclear structure, we calculate the longitudinal spin asymmetries in polarized tagged DIS and study the dependence on the measured proton momentum. We consider the asymmetries formed with all three deuteron spin states $(\pm 1, 0)$ and the two maximum-spin states only (± 1). We show that the proton momentum can be used to select pure S-wave configurations and eliminate D-wave depolarization. We discuss how free neutron spin structure can be extracted through pole extrapolation of the asymmetries. Details will be provided in a forthcoming article [23].

2. Spin asymmetries in polarized tagged DIS

Polarized tagged DIS with deuteron 4-momentum p_D and 4-momentum transfer $q \equiv p_e - p_e'$ is described by the invariant differential cross section (see Fig. 1a)

$$\mathrm{d}\sigma[eD \to e'Xp] = \mathcal{F}\,\mathrm{d}x\,\mathrm{d}Q^2\,\mathrm{d}\Gamma_p, \tag{1}$$

$$\mathcal{F} \equiv \mathcal{F}(x, Q^2; \{p_p\}; \mathrm{pol}_e, \mathrm{pol}_D), \tag{2}$$

where $x \equiv Q^2/(p_D q)$ and $Q^2 \equiv -q^2$ are the usual DIS variables, $\{p_p\}$ denotes a set of variables describing the measured proton momentum, $\mathrm{d}\Gamma_p$ is the invariant phase space element in the proton momentum, and "pol_e" and "pol_D" denote generic variables specifying the initial electron and deuteron polarization. As generally for semi-inclusive DIS, it is convenient to describe the process in a frame where the 3-vectors $\boldsymbol{p}_D$ and $\boldsymbol{q}$ are collinear along the z-axis (see Fig. 1b). We specify the particle momenta in this frame by their LF components $p^\pm \equiv p^0 \pm p^3$, $\boldsymbol{p_T} \equiv (p^1, p^2)$. The proton is described by its plus momentum fraction and transverse momentum

$$\alpha_p \equiv 2p_p^+/p_D^+ \quad (0 < \alpha_p < 2), \quad \boldsymbol{p}_{pT}, \tag{3}$$

with $\mathrm{d}\Gamma_p = (\mathrm{d}\alpha_p/\alpha_p)\,\mathrm{d}^2 p_{pT}$. The typical ranges of these variables are $|\alpha_p - 1| \lesssim 0.1$ and $|\boldsymbol{p}_{pT}| \lesssim 100$ MeV, corresponding to proton 3-momenta $|\boldsymbol{p}_p| \lesssim 100$ MeV in the deuteron rest frame. The dependence of the cross section on the proton azimuthal angle ϕ_p is kinematic and can be established on general grounds; the decomposition will be presented elsewhere [23]. In the following we consider the azimuthally integrated cross section,

$$\mathrm{d}\sigma \equiv \left[\int \mathrm{d}\phi_p \mathcal{F}\right] \mathrm{d}x\,\mathrm{d}Q^2\,(\mathrm{d}\alpha_p/\alpha_p)\,|\boldsymbol{p}_{pT}|\,\mathrm{d}|\boldsymbol{p}_{pT}|, \tag{4}$$

which is sufficient for neutron spin structure measurements.

The polarization variables in Eq. (1) have to be specified depending on the experimental setup. We consider a collider experiment in which the electron and deuteron beams move in opposite directions along the same axis in the laboratory (zero crossing angle). The electron entering the scattering process is in a spin state quantized along the beam axis with projections $\Lambda_e = \pm\frac{1}{2}$. The deuteron is in a spin state quantized along the beam axis with projections $\Lambda_D = (1, 0, -1)$; combinations of these pure states correspond to spin ensembles with longitudinal vector and tensor polarization. We denote the cross section in the pure spin states by

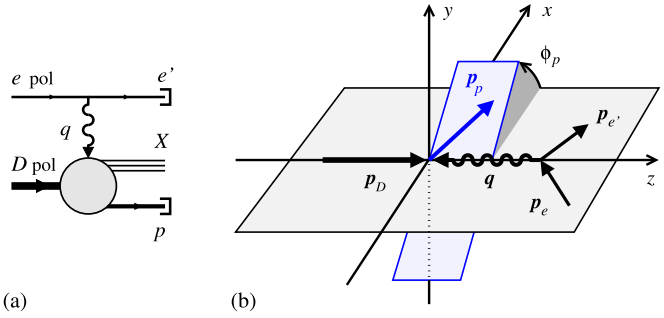

Fig. 1. (a) Polarized electron-deuteron DIS with proton tagging, $e + D \to e' + X + p$. (b) Momenta in the photon-deuteron collinear frame.

$$\mathrm{d}\sigma \equiv \mathrm{d}\sigma(\Lambda_e, \Lambda_D). \tag{5}$$

The beam polarizations in the laboratory frame determine the effective polarizations of the electron and deuteron in the photon-deuteron collinear frame; the corresponding kinematic factors (depolarization factors) are given below.

Experiments measure differences and sums of the cross sections in different electron and deuteron polarization states and their ratios (spin asymmetries). The "polarized" cross section is calculated as the difference between the $\Lambda_D = \pm 1$ deuteron spin states,[1]

$$\mathrm{d}\sigma_\parallel \equiv \tfrac{1}{4}[\mathrm{d}\sigma(\tfrac{1}{2}, 1) - \mathrm{d}\sigma(-\tfrac{1}{2}, 1) - \mathrm{d}\sigma(\tfrac{1}{2}, -1) + \mathrm{d}\sigma(-\tfrac{1}{2}, -1)]. \tag{6}$$

"Unpolarized" cross sections can be formed in two ways: (i) as the sum of all three deuteron spin states $(\Lambda_D = \pm 1, 0)$,

$$\mathrm{d}\sigma_3 \equiv \tfrac{1}{6} \sum_{\Lambda_e = \pm 1/2} [\mathrm{d}\sigma(\Lambda_e, +1) + \mathrm{d}\sigma(\Lambda_e, -1) + \mathrm{d}\sigma(\Lambda_e, 0)]; \tag{7}$$

(ii) as the sum of the two maximum-spin states only $(\Lambda_D = \pm 1)$, which enter in the polarized cross section Eq. (6),

$$\mathrm{d}\sigma_2 \equiv \tfrac{1}{4} \sum_{\Lambda_e = \pm 1/2} [\mathrm{d}\sigma(\Lambda_e, +1) + \mathrm{d}\sigma(\Lambda_e, -1)]. \tag{8}$$

The combination Eq. (8) implies a nonzero tensor polarization of the deuteron ensemble. Correspondingly, one can define the "three-state" and "two-state" tagged spin asymmetries as

$$A_{\parallel,3} \equiv \frac{\mathrm{d}\sigma_\parallel}{\mathrm{d}\sigma_3}, \qquad A_{\parallel,2} \equiv \frac{\mathrm{d}\sigma_\parallel}{\mathrm{d}\sigma_2}. \tag{9}$$

They depend on x and Q^2 and the proton momentum variables α_p and $|\boldsymbol{p}_{pT}|$ [ϕ_p is integrated out, Eq. (4)],

$$A_{\parallel,i}(x, Q^2; \alpha_p, |\boldsymbol{p}_{pT}|) \qquad (i = 3, 2). \tag{10}$$

In the following we compute the tagged asymmetries in an approach that separates nuclear and nucleonic structure, study their dependence on the proton momentum, and assess their usefulness for neutron spin structure extraction.

[1] In fully inclusive DIS the spin dependence of the cross section is entirely through double-spin dependent terms $\propto \Lambda_e \Lambda_D$, and it is sufficient to take the difference in the electron or deuteron spin alone, with the other spin remaining fixed. In tagged DIS the cross section can have also single-spin dependent terms $\propto \Lambda_e$ and $\propto \Lambda_D$, and it is necessary to take the double difference in the electron and deuteron spins in order to isolate the double-spin dependent terms.

3. Deuteron light-front wave function

To calculate the tagged DIS cross section we use methods of LF nuclear structure. The quantization scheme is unique in that the effects of energy nonconservation (or 4-momentum nonconservation) in intermediate states remain finite in the high-energy limit and enables a practical description of high-energy scattering from composite systems [22]. The technique is summarized in Ref. [24]; here we only describe the aspects specific to the spin degrees of freedom. The calculation is performed in the photon-deuteron collinear frame (see Fig. 1b). The deuteron is described by a wave function in nucleonic degrees of freedom at fixed LF time (see Fig. 2a). The nucleon spin states are chosen as LF helicity states (LF boosts of rest-frame spin states quantized along the z-axis [25,26]) with helicity quantum numbers $\lambda_p, \lambda_n = \pm\frac{1}{2}$; the deuteron LF helicity $\lambda_D = (1, 0, -1)$ is identical to its ordinary spin projection on the z-axis (its transverse momentum is zero). The LF wave function is constructed from a rotationally covariant 3-dimensional wave function in the center-of-mass (CM) frame of the pn pair [27]

$$\Psi(\alpha_p, \boldsymbol{p}_{pT}; \lambda_p, \lambda_n|\lambda_D) = \sum_{\mu_p,\,\mu_n} \widetilde{\Psi}(\boldsymbol{k}, \mu_p, \mu_n|\lambda_D) \times U^*(\boldsymbol{k}, \mu_p, \lambda_p)\, U^*(-\boldsymbol{k}, \mu_n, \lambda_n), \tag{11}$$

$$\widetilde{\Psi}(\boldsymbol{k}, \mu_p, \mu_n|\lambda_D) \equiv \frac{\epsilon^a(\lambda_D)}{\sqrt{2}} \left[\delta^{ab} f_0(k) + \left(\frac{3k^a k^b}{|\boldsymbol{k}|^2} - \delta^{ab} \right) \frac{f_2(k)}{\sqrt{2}} \right] \times\ \chi^\dagger(\mu_n) \left[\sigma^b (i\sigma^2) \right] \chi^*(\mu_p), \tag{12}$$

$$U(\boldsymbol{k}, \mu_p, \lambda_p) \equiv \chi^\dagger(\mu_p) \left[\frac{E + k^3 + m + \boldsymbol{k}_T \boldsymbol{\sigma}_T \sigma^3}{\sqrt{2(E + k^3)(E + m)}} \right] \chi(\lambda_p), \tag{13}$$

$$U(-\boldsymbol{k}, \mu_n, \lambda_n) \equiv [\text{same with } \boldsymbol{k} \to -\boldsymbol{k};\ \ \mu_p, \lambda_p \to \mu_n, \lambda_n]. \tag{14}$$

Here $\boldsymbol{k} = (\boldsymbol{k}_T, k^3)$ is the CM momentum of the pn pair and related to the LF momentum variables by (m is nucleon mass)

$$\alpha_p = 1 + k^3/E, \qquad E = \sqrt{m^2 + |\boldsymbol{k}|^2}, \qquad \boldsymbol{p}_{pT} = \boldsymbol{k}_T. \tag{15}$$

$\widetilde{\Psi}$ is the rotationally covariant wave function in the CM frame; it is formulated in canonical nucleon spin states with quantum numbers $\mu_p, \mu_n = \pm\frac{1}{2}$. σ^a $(a = 1, 2, 3)$ are the Pauli spin matrices; $\chi(\nu)$ $(\nu = \mu_p, \mu_n, \lambda_p, \lambda_n)$ are the two-component spinors for spin projection $\nu = \pm\frac{1}{2}$ on the z-axis, $\chi(\frac{1}{2}) = (1, 0)^T$, $\chi(-\frac{1}{2}) = (0, 1)^T$; $\boldsymbol{\epsilon}(\lambda_D)$ is the spin-1 polarization vector for spin projection λ_D, $\boldsymbol{\epsilon}(\pm1) = \frac{1}{\sqrt{2}}(\mp1, -i, 0)^T$, $\boldsymbol{\epsilon}(0) = (0, 0, 1)^T$. The CM frame wave function Eq. (12) involves the S- and D-waves of the pn pair. They are described by the radial wave functions $f_0(k)$ and $f_2(k)$, $k \equiv |\boldsymbol{k}|$, which are normalized as

$$4\pi \int_0^\infty \frac{\mathrm{d}k\, k^2}{E(k)} [f_0^2(k) + f_2^2(k)] \ = \ 1. \tag{16}$$

In Eqs. (11)–(14) U are the momentum-dependent Melosh rotations connecting the canonical nucleon spin states with the LF helicity states (U^* denotes the complex conjugate). The construction Eqs. (11)–(13) effectively implements rotational invariance in the LF calculation and permits a simple description of the deuteron spin structure in this context [14,27,28].

The radial wave functions can be obtained by solving the 2-body bound-state equation with pn interactions at fixed LF time

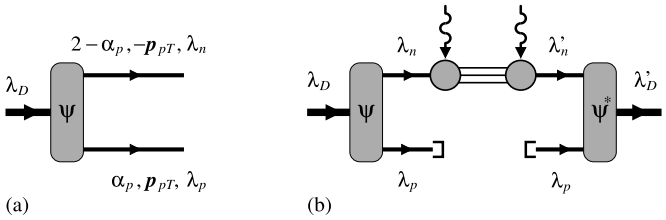

Fig. 2. (a) Deuteron LF wave function. (b) Polarized tagged DIS cross section in impulse approximation.

[14,29]. Alternatively, one can approximate them by the nonrelativistic wave functions as

$$f_L(k) \overset{\text{app.}}{=} \sqrt{E(k)}\, f_{L,\,\mathrm{nr}}(k) \qquad (L = 0, 2); \tag{17}$$

the factor arises from the normalization Eq. (16). Equation (17) is reliable at all momenta of interest here [14,24]; in the numerical studies we use it with the AV18 wave functions [30].

4. Deuteron light-front spectral function

We calculate the tagged DIS cross section in the impulse approximation, in which the DIS final state and the spectator evolve independently after the scattering process (see Fig. 2b). The general expressions for the cross section and scattering tensor are summarized in Ref. [24]. The polarized deuteron scattering tensor is factorized in the polarized neutron scattering tensor and the deuteron LF spectral function,

$$\mathcal{S}(\alpha_p, \boldsymbol{p}_{pT}; \lambda_n', \lambda_n|\lambda_D', \lambda_D) \ \equiv\ \frac{1}{2 - \alpha_p} \times \sum_{\lambda_p} \Psi^*(\alpha_p, \boldsymbol{p}_{pT}; \lambda_p, \lambda_n'|\lambda_D')\, \Psi(\alpha_p, \boldsymbol{p}_{pT}; \lambda_p, \lambda_n|\lambda_D). \tag{18}$$

It describes the conditional probability density of the neutron in the deuteron when removing a proton with LF momentum α_p and $\boldsymbol{p}_{pT}$, and is normalized as

$$\sum_{\lambda_n} \int_0^2 \frac{\mathrm{d}\alpha_p}{\alpha_p} \int \mathrm{d}^2 p_{pT}\, \mathcal{S}(\alpha_p, \boldsymbol{p}_{pT}; \lambda_n, \lambda_n|\lambda_D', \lambda_D) \ = \ \delta_{\lambda_D' \lambda_D}. \tag{19}$$

The general spectral function Eq. (18) is a matrix in the LF helicities of the external deuteron and intermediate neutron states. In the calculation of the cross section, the deuteron LF helicities are averaged over with the deuteron spin density matrix, which describes the effective deuteron polarization in LF helicities, taking into account that the experimental polarization is along the beam axis (see Sec. 2). The neutron helicities are averaged over with the spin structure of the neutron scattering tensor. In the particular case of the ϕ_p-integrated cross sections with the longitudinal deuteron polarization described in Sec. 2, the result can be expressed in terms of three distinct LF helicity projections of the spectral function Eq. (18) [23]:

$$\mathcal{S}_U = \sum_{\lambda_D \lambda_D'} (\rho_U)_{\lambda_D \lambda_D'} \sum_{\lambda_n \lambda_n'} \mathcal{S}(\lambda_n', \lambda_n|\lambda_D', \lambda_D)\, \delta_{\lambda_n \lambda_n'}, \tag{20}$$

$$\Delta\mathcal{S}_S = \sum_{\lambda_D \lambda_D'} (\rho_S)_{\lambda_D \lambda_D'} \sum_{\lambda_n \lambda_n'} \mathcal{S}(\lambda_n', \lambda_n|\lambda_D', \lambda_D)\, (2\lambda_n)\, \delta_{\lambda_n \lambda_n'}, \tag{21}$$

$$\mathcal{S}_T = \sum_{\lambda_D \lambda_D'} (\rho_T)_{\lambda_D \lambda_D'} \sum_{\lambda_n \lambda_n'} \mathcal{S}(\lambda_n', \lambda_n|\lambda_D', \lambda_D)\, \delta_{\lambda_n \lambda_n'}. \tag{22}$$

Here $\rho_{U,S,T}$ are the spin-1 density matrices describing an unpolarized, vector-polarized, and tensor-polarized ensemble quantized along the z-axis,

$$(\rho_U)_{\lambda_D\lambda'_D} = \tfrac{1}{3}\mathrm{diag}(1,1,1), \tag{23}$$

$$(\rho_S)_{\lambda_D\lambda'_D} = \tfrac{1}{2}\mathrm{diag}(1,0,-1), \tag{24}$$

$$(\rho_T)_{\lambda_D\lambda'_D} = \tfrac{1}{6}\mathrm{diag}(1,-2,1). \tag{25}$$

The functions $\mathcal{S}_U, \Delta\mathcal{S}_S$ and $\mathcal{S}_T$ depend on the proton LF momentum variables α_p and $|\boldsymbol{p}_{pT}|$. $\mathcal{S}_U$ describes the LF helicity-independent probability of neutrons in an unpolarized deuteron ensemble; $\mathcal{S}_T$ describes the LF helicity-independent probability of neutrons in a tensor-polarized deuteron ensemble; $\Delta\mathcal{S}_S$ describes the LF helicity-dependent probability of neutrons in a vector-polarized deuteron ensemble. Their interpretation is similar to that of the unpolarized and helicity-polarized parton densities in the nucleon and can be developed further along these lines [23]. We evaluate the functions by using the explicit expression of the deuteron LF wave function and performing the sums over the LF helicities and obtain [23]

$$\mathcal{S}_U(\alpha_p, |\boldsymbol{p}_{pT}|) = \frac{1}{2-\alpha_p}\left(f_0^2 + f_2^2\right), \tag{26}$$

$$\Delta\mathcal{S}_S(\alpha_p, |\boldsymbol{p}_{pT}|) = \frac{1}{2-\alpha_p}\left(f_0 - \frac{f_2}{\sqrt{2}}\right)\left(C_0 f_0 - \frac{C_2 f_2}{\sqrt{2}}\right), \tag{27}$$

$$C_0 = 1 - \frac{(E+k^3)|\boldsymbol{k}_T|^2}{(E+m)(m^2+|\boldsymbol{k}_T|^2)}, \tag{28}$$

$$C_2 = 1 - \frac{(E+2m)(E+k^3)|\boldsymbol{k}_T|^2}{(m^2+|\boldsymbol{k}_T|^2)|\boldsymbol{k}|^2}, \tag{29}$$

$$\mathcal{S}_T(\alpha_p, |\boldsymbol{p}_{pT}|) = \frac{1}{2-\alpha_p} C_T \left(-2f_0 - \frac{f_2}{\sqrt{2}}\right)\frac{f_2}{\sqrt{2}}, \tag{30}$$

$$C_T = 1 - \frac{3|\boldsymbol{k}_T|^2}{2|\boldsymbol{k}|^2}, \tag{31}$$

where $f_{0,2} \equiv f_{0,2}(k)$ are the radial wave functions of Eq. (12). The factors C_0 and C_2 in Eq. (27), and C_T in Eq. (30), arise from the contraction of the Melosh rotations Eq. (13) and contain the relativistic spin effects in the neutron distributions in the polarized deuteron. They play an essential role in the proton momentum dependence of the polarized tagged DIS cross section (see below).

The deuteron spectral function Eq. (26) satisfies sum rules for the total baryon number and the total LF momentum of the neutron, obtained by integrating over the proton momentum,

$$\int \frac{d\alpha_p}{\alpha_p}\int d^2p_{pT}\,\mathcal{S}_U(\alpha_p, \boldsymbol{p}_{pT}) \times \left\{\begin{array}{c} 1 \\ (2-\alpha_p)\end{array}\right\} = \left\{\begin{array}{c} 1 \\ 1\end{array}\right\}. \tag{32}$$

They follow from the normalization condition Eq. (19) and the symmetry of the deuteron wave function under $\alpha_p \to 2-\alpha_p$, which is a consequence of the rotational invariance encoded in Eq. (12). The sum rules indicate that a consistent description of deuteron structure in terms of nucleon degrees of freedom is achieved in the impulse approximation.

5. Deuteron structure in spin asymmetries

Using the deuteron spectral functions we compute the longitudinal spin asymmetries of the azimuthally integrated tagged DIS cross section (see Sec. 2). We consider the DIS limit $Q^2 \to \infty$, x fixed, and neglect power-suppressed terms in the kinematic factors and the spin-dependent cross section (g_2 structure function). The result for the three- and two-state asymmetries Eq. (9) can be expressed in simple form as [here $i = 3, 2$]

$$A_{\parallel,i}(x, Q^2; \alpha_p, |\boldsymbol{p}_{pT}|) = A_{\parallel n}(\tilde{x}, Q^2)\,\mathcal{D}_i(\alpha_p, |\boldsymbol{p}_{pT}|), \tag{33}$$

$$A_{\parallel n}(\tilde{x}, Q^2) = \frac{D_\parallel\, g_{1n}(\tilde{x}, Q^2)}{2(1+\epsilon R_n)F_{1n}(\tilde{x}, Q^2)}. \tag{34}$$

$A_{\parallel n}$ is the longitudinal spin asymmetry for DIS on the free neutron. It is given in terms of the polarized and unpolarized neutron structure functions, g_{1n} and F_{1n}, and the neutron L/T ratio R_n. The neutron functions are evaluated at the modified x-value

$$\tilde{x} = x/(2-\alpha_p), \tag{35}$$

where $2-\alpha_p$ is the plus momentum fraction of the active neutron, whose value is fixed by the α_p of the tagged proton. In Eq. (34) ϵ is the virtual photon polarization parameter; $D_\parallel$ is the depolarization factor describing the effective polarization in the photon-deuteron collinear frame induced by the experimental polarization along the beam axis (see Sec. 2),

$$\epsilon = \frac{1-y}{1-y+y^2/2}, \qquad D_\parallel = \frac{2y(1-y/2)}{1-y+y^2/2}; \tag{36}$$

the scaling variable $y \equiv (p_D q)/(p_D p_e)$ is the same for DIS on the deuteron and the free neutron up to power-suppressed corrections (we do not distinguish between the two in the notation). The typical magnitude of $A_{\parallel n}$ is a few $\times 10^{-2}$ for $\tilde{x} \gtrsim 10^{-2}$ and $y = \mathcal{O}(1)$ [21]. The deuteron structure effects in Eq. (33) are contained in the factors $\mathcal{D}_i$ ($i = 3, 2$), which depend on the proton variables α_p and $|\boldsymbol{p}_{pT}|$. They play the role of a "dynamical depolarization factor" specific to the deuteron configuration selected by the tagged proton momentum. For the three-state and two-state asymmetries, Eq. (9), they are obtained as

$$\mathcal{D}_3(\alpha_p, |\boldsymbol{p}_{pT}|) \equiv \frac{\Delta\mathcal{S}_S(\alpha_p, |\boldsymbol{p}_{pT}|)}{\mathcal{S}_U(\alpha_p, |\boldsymbol{p}_{pT}|)}, \tag{37}$$

$$\mathcal{D}_2(\alpha_p, |\boldsymbol{p}_{pT}|) \equiv \frac{\Delta\mathcal{S}_S(\alpha_p, |\boldsymbol{p}_{pT}|)}{[\mathcal{S}_U + \mathcal{S}_T](\alpha_p, |\boldsymbol{p}_{pT}|)}. \tag{38}$$

The numerator in both cases is the vector-polarized spectral function Eq. (21). The denominator in the three-state asymmetry is the unpolarized spectral function Eq. (20); in the two-state asymmetry there is a contribution of the tensor-polarized spectral function Eq. (22), because the sum of ± 1 spin states only (without the 0 state) corresponds to a spin ensemble with nonzero tensor polarization.

We evaluate the deuteron structure factors Eqs. (37) and (38) using the explicit expressions for the spectral functions Eqs. (26)–(31). Important differences between $\mathcal{D}_3$ and $\mathcal{D}_2$ can be deduced from the analytic expressions. (a) $\mathcal{D}_2$ is bounded by unity,

$$-1 \le \mathcal{D}_2 \le 1. \tag{39}$$

No such bound is found for $\mathcal{D}_3$, which attains absolute values larger than unity. (b) $\mathcal{D}_2$ is equal to unity at zero proton transverse momentum and arbitrary plus momentum,

$$\mathcal{D}_2(\alpha_p, |\boldsymbol{p}_{pT}| = 0) = 1 \qquad (\alpha_p \text{ arbitrary}). \tag{40}$$

This happens because the factors C_0, C_2 and C_T in Eqs. (28), (29) and (31) become unity at $\boldsymbol{k}_T = 0$ [the Melosh rotations are trivial at zero transverse momentum, $U(\boldsymbol{k}_T = 0) = 1$, cf. Eqs. (13) and (14)]. In contrast, $\mathcal{D}_3$ is equal to unity only at $|\boldsymbol{p}_{pT}| = 0$ and $\alpha_p = 1$. (c) At small proton momenta, $|\alpha_p - 1| \ll 1$ and $|\boldsymbol{p}_{pT}| \ll m$,

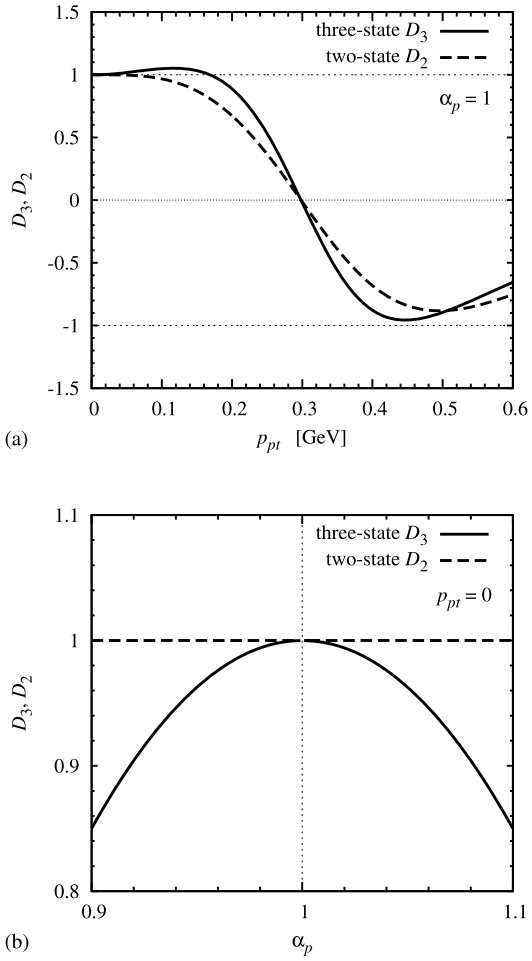

Fig. 3. Deuteron structure factors $\mathcal{D}_3$ (three-state asymmetry) and $\mathcal{D}_2$ (two-state asymmetry) in polarized tagged DIS, Eqs. (37) and (38). (a) As functions of $p_{pT} \equiv |\boldsymbol{p}_{pT}|$, for fixed $\alpha_p = 1$. (b) As functions of α_p in the vicinity of $\alpha_p = 1$, for fixed $p_{pT} = 0$.

corresponding to $|\boldsymbol{k}| \ll m$, the D-wave affects $\mathcal{D}_2$ only at quadratic order, but $\mathcal{D}_3$ already at linear order,

$$\left.\begin{aligned} \mathcal{D}_2 &= 1 + \text{terms } f_2^2/f_0^2 \\ \mathcal{D}_3 &= 1 + \text{terms } f_2/f_0 \end{aligned}\right\} \quad (|\boldsymbol{k}| \ll m). \tag{41}$$

This can be demonstrated by expanding the factors C_0 and C_2 in Eqs. (28) and (29) in $|\boldsymbol{k}|/m$, and then expanding the spectral function ratios in Eqs. (37) and (38) in f_2/f_0.

Fig. 3a shows the deuteron structure factors Eqs. (37) and (38) as functions of $|\boldsymbol{p}_{pT}|$ for fixed $\alpha_p = 1$. One observes: (a) Both $\mathcal{D}_3$ and $\mathcal{D}_2$ are unity at $\alpha_p = 1$ and $|\boldsymbol{p}_{pT}| = 0$, where $|\boldsymbol{k}| = 0$ and only the S-wave is present. (b) $\mathcal{D}_3$ and $\mathcal{D}_2$ remain close to unity for $|\boldsymbol{p}_{pT}| \lesssim 150$ MeV, where the S-wave dominates. The D-wave contribution raises $\mathcal{D}_3$ above unity but lowers $\mathcal{D}_2$, in accordance with the bound Eq. (39), showing the effect of the tensor polarized structure in $\mathcal{D}_2$. (c) Both $\mathcal{D}_3$ and $\mathcal{D}_2$ decrease significantly at $|\boldsymbol{p}_{pT}| \gtrsim 150$ MeV and pass through zero at $|\boldsymbol{p}_{pT}| \approx 300$ MeV, where the combination $(f_0 - f_2/\sqrt{2})$ vanishes. Both become negative at larger momenta, where the D-wave dominates.

Fig. 3b shows the deuteron structure factors as functions of α_p near $\alpha_p = 1$ for fixed $|\boldsymbol{p}_{pT}| = 0$. One observes that $\mathcal{D}_2 = 1$ in accordance with Eq. (40), whereas $\mathcal{D}_3$ shows a sizable variation in $\alpha_p - 1$. Altogether we find that at small proton momenta $\mathcal{D}_2$ is much closer to unity than $\mathcal{D}_3$.

In the present analysis we consider the longitudinal spin asymmetries $A_{\parallel,i}$ $(i = 2, 3)$ in the DIS limit $Q^2 \gg m^2$ and neglect power corrections (leading-twist approximation). In this approximation the $A_{\parallel,i}$ only involve the g_{1n} structure function; the contribution from g_{2n} is power-suppressed [1]; and the variables characterizing the DIS process on the neutron are taken at their $Q^2 \gg m^2$ values. At this level of accuracy the effects of interactions in the transverse component of the electromagnetic current operator in LF quantization can generally be neglected, enabling a consistent description of deuteron structure with nucleon degrees of freedom only [4]; see also Ref. [31]. This is seen e.g. in the fact that the deuteron spectral function in the impulse approximation satisfies the LF momentum sum rule Eq. (32), which in turn ensures the momentum sum rule for the deuteron structure function F_{2D}, provided that the kinematic limits are taken at $Q^2 \gg m^2$ [4,24]. The present analysis could be extended to calculate the longitudinal spin asymmetries including power corrections and the contributions from g_{2n}, or to calculate the transverse spin asymmetries, which are altogether power-suppressed. At this level of accuracy the interaction effects in the transverse current component could no longer be neglected, and new considerations would be needed in order to construct a consistent description with nucleons only — implementation of rotational invariance in LF calculations with fixed particle number, or the so-called angular conditions on the current operators or matrix elements. These problems have been studied extensively in the context of elastic scattering on the deuteron; see Refs. [27,31–34] and references therein; the methods could be adapted to the case of DIS beyond leading power accuracy.

6. Neutron spin structure from pole extrapolation

The tagged DIS cross section is generally affected by initial-state nuclear modifications of the structure functions and final-state interactions of the DIS products with the spectator. These effects can be described by dynamical models and added to the impulse approximation [24,35]. An alternative approach is to eliminate them using the analytic properties of the proton momentum dependence [15]. Analytic continuation in the proton momentum can select pn configurations at asymptotically large distances, where the neutron is effectively free. This approach does not require input beyond the impulse approximation and permits model-independent extraction of free neutron structure from tagged DIS. Its feasibility in the unpolarized case was studied in Refs. [15,24]; here we apply it to the polarized case.

For the study of analytic properties one regards the deuteron wave function as a function of the invariant mass of the pn pair,

$$M_{pn}^2 = \frac{4(|\boldsymbol{p}_{pT}|^2 + m^2)}{\alpha_p(2 - \alpha_p)} = 4(|\boldsymbol{k}|^2 + m^2), \tag{42}$$

which depends on α_p and $|\boldsymbol{p}_{pT}|$ and takes values $M_{pn}^2 \geq 4m^2$ for physical proton momenta. The wave function has a pole singularity of the type (M_D is the deuteron mass; we suppress the spin structure for the moment)

$$\Psi(\alpha_p, |\boldsymbol{p}_{pT}|) = \frac{\Phi}{M_{pn}^2 - M_D^2} + [\text{less singular}], \tag{43}$$

which corresponds to pn configurations of asymptotically large transverse spatial separation, outside the range of the nucleon interaction. The singularity lies outside the physical region of proton momenta because $M_{pn}^2 \geq 4m^2 > M_D^2$ but can be reached by analytic continuation in $|\boldsymbol{p}_{pT}|^2$ to unphysical negative values,

$$|\boldsymbol{p}_{pT}|^2 \to -a_T^2, \qquad a_T^2 \equiv m^2 - \alpha_p(2 - \alpha_p)M_D^2/4. \tag{44}$$

The minimum value of a_T^2 occurs at $\alpha_p = 1$ and is $a_T^2 = m^2 - M_D^2/4 = m\epsilon_D + \mathcal{O}(\epsilon_D^2) = a^2$, where $\epsilon_D \equiv 2m - M_D$ is the deuteron binding energy and $a^2 \equiv m\epsilon_D$ is the inverse squared Bethe-Peierls radius of the deuteron. Because of the small value of the deuteron binding energy ($\epsilon_D = 2.2$ MeV) the singularity is very close to the physical region and can be reached by extrapolation in $|\boldsymbol{p}_{pT}|^2$. This opens a practical way of accessing non-interacting large-size pn configurations in the deuteron through analytic continuation. In the representation of the deuteron LF wave function in terms of the 3-dimensional CM frame wave function, Eq. (12), the pole Eq. (43) appears through the pole of the S-wave radial function

$$f_0(k) \;=\; \frac{\sqrt{m}\,\Gamma}{|\boldsymbol{k}|^2 + a^2} \;+\; [\text{less singular}], \tag{45}$$

which is a general feature of the weakly bound system. This illustrates the close correspondence between the LF and the nonrelativistic description of the two-body bound state.

On general grounds, the tagged DIS cross section as a function of the proton momentum has a pole $\sim (M_{pn}^2 - M_D^2)^{-2}$, corresponding to scattering from a large-size pn pair. The residue of this pole is, up to a constant factor, given by the *free neutron cross section*. The pole is contained entirely in the impulse approximation to the tagged DIS cross section and is a feature of the deuteron spectral function (see Sec. 4). Final-state interactions do not modify the pole and affect only the less singular terms of the momentum dependence, because they involve momentum loop integrals [15, 24]. To extract the free neutron structure functions, one measures the tagged DIS cross section for fixed α_p as a function of $|\boldsymbol{p}_{pT}|^2$ in the physical region $|\boldsymbol{p}_{pT}|^2 > 0$, removes the pole factor, and extrapolates the residue to $|\boldsymbol{p}_{pT}|^2 \to -a_T^2$ according to Eq. (44) (pole extrapolation). For unpolarized DIS the procedure was studied in detail in Refs. [15,24].

For polarized DIS the pole extrapolation can be performed at the level of the spin asymmetries. One measures the tagged spin asymmetries for fixed α_p as functions of $|\boldsymbol{p}_{pT}|^2$ for $|\boldsymbol{p}_{pT}|^2 > 0$. The pole factors $\sim (M_{pn}^2 - M_D^2)^{-2}$ in the cross sections cancel between the numerator and denominator of the spin asymmetries, as can be seen in the ratios of spectral functions, Eqs. (37) and (38), so that the asymmetries are smooth functions in the limit $|\boldsymbol{p}_{pT}|^2 \to -a_T^2$. The free neutron spin asymmetry is then obtained by extrapolating the measured tagged deuteron asymmetries to $|\boldsymbol{p}_{pT}|^2 = -a_T^2$ and removing the deuteron structure factor. Specifically, using the two-state deuteron asymmetry,

$$A_{\parallel n}(\tilde{x},\, Q^2) \;=\; \frac{A_{\parallel,2}(x,\, Q^2; \alpha_p, |\boldsymbol{p}_{pT}|^2 \to -a_T^2)}{\mathcal{D}_2(\alpha_p, |\boldsymbol{p}_{pT}|^2 \to -a_T^2)}, \tag{46}$$

$$\mathcal{D}_2(\alpha_p, |\boldsymbol{p}_{pT}|^2 \to -a_T^2) \;=\; 1 \;+\; \frac{(\alpha_p - 1)^2}{2(2 - \alpha_p)} + \mathcal{O}\left(\frac{\epsilon_D}{m}\right). \tag{47}$$

Eq. (47) is the deuteron structure factor Eq. (38) extrapolated to $|\boldsymbol{p}_{pT}|^2 = -a_T^2$; the extrapolation is performed using the explicit expressions for the spectral functions Eqs. (26)–(31). A similar expression can be derived for the three-state asymmetry.

In practice, the pole extrapolation can be performed by measuring the tagged deuteron asymmetry over a range $|\boldsymbol{p}_{pT}| \lesssim 100$ MeV and extrapolating the data using low-order polynomial fits [15]. It is convenient to use the two-state rather than the three-state asymmetry, as the former exhibits a much weaker dependence on the proton momentum at small momenta (cf. Sec. 5). The two-state asymmetry also has the advantage that only preparation of the ± 1 deuteron spin states is required, reducing the systematic uncertainty. First simulations of the asymmetry measurements with projected experimental uncertainties at EIC have been described in Ref. [21].

For a full assessment of the feasibility of the pole extrapolation one should estimate also the effects of final-state interactions between the tagged proton and the DIS products. Such interactions can modify the tagged DIS cross section at physical proton momenta but are suppressed at the pole; they can thus affect the practical performance of the pole extrapolation but not its theoretical result. Detailed studies have shown that in the unpolarized tagged cross section, Eq. (7), final-state interaction corrections to the impulse approximation are moderate at momenta $|\boldsymbol{p}_{pT}| \lesssim 100$ MeV and do not impede the pole extrapolation [24]. The longitudinally polarized cross section, Eq. (6), is similar to the unpolarized one in the sense that in both cases the impulse approximation is given by the square of the dominant S-wave amplitude. One can therefore expect that the final-state interaction effects at momenta $|\boldsymbol{p}_{pT}| \lesssim 100$ MeV are not substantially larger in the longitudinally polarized cross section than in the unpolarized one. Quantitative estimates could be obtained by generalizing the methods of Ref. [24], but require extensive modeling of the dynamical input (polarized neutron fragmentation, spin-dependent rescattering).

7. Conclusions and extensions

The main conclusions of the present study can be summarized as follows: (a) The measured proton momentum in tagged DIS effectively controls the spin structure of the pn configuration in deuteron. This feature can be used to select pure S-wave configurations and eliminate D-wave depolarization. (b) The two-state longitudinal spin asymmetry has simpler properties than the three-state asymmetry in tagged DIS. In the two-state asymmetry the nuclear structure factor is bounded by unity, and equal to unity at $|\boldsymbol{p}_{pT}| = 0$, and the D-wave contributions vanish rapidly at small proton momenta. (c) The free neutron spin asymmetry can be extracted by pole extrapolation of the tagged spin asymmetries in $|\boldsymbol{p}_{pT}|^2$. The method effectively accesses non-interacting large-size pn configurations through analytic continuation. The extrapolation of the asymmetries is technically simple because the pole factors cancel between numerator and denominator. In sum, DIS on the polarized deuteron with proton tagging permits control of the pn configuration during the polarized DIS process (momentum, spin, interactions) and enables new ways of neutron spin structure extraction.

The theoretical methods for high-energy scattering on the polarized deuteron with spectator tagging described here can be applied and extended to several other types of measurements of interest [23]. This includes tagged DIS with transverse deuteron polarization; azimuthal asymmetries and tensor-polarized tagged structure functions; tagged measurements of hard exclusive processes on the neutron such as deeply-virtual Compton scattering; and the use of tagging for studies of nuclear modifications of partonic structure.

Acknowledgements

This material is based upon work supported by the U.S. Department of Energy, Office of Science, Office of Nuclear Physics under contract DE-AC05-06OR23177. It is partly based upon work supported by Jefferson Lab's 2014/2015 Laboratory-Directed Research and Development Project "Physics potential of polarized light ions with EIC@JLab" (see Ref. [20]). W.C. acknowledges the hospitality of the Jefferson Lab Theory Center.

References

[1] M. Anselmino, A. Efremov, E. Leader, The theory and phenomenology of polarized deep inelastic scattering, Phys. Rep. 261 (1995) 1–124, https://doi.org/10.1016/0370-1573(95)00011-5, arXiv:hep-ph/9501369; Erratum: Phys. Rep. 281 (1997) 399.

[2] S.E. Kuhn, J.P. Chen, E. Leader, Spin structure of the nucleon — status and recent results, Prog. Part. Nucl. Phys. 63 (2009) 1–50, https://doi.org/10.1016/j.ppnp.2009.02.001, arXiv:0812.3535.

[3] C.A. Aidala, S.D. Bass, D. Hasch, G.K. Mallot, The spin structure of the nucleon, Rev. Mod. Phys. 85 (2013) 655–691, https://doi.org/10.1103/RevModPhys.85.655, arXiv:1209.2803.

[4] L.L. Frankfurt, M.I. Strikman, Hard nuclear processes and microscopic nuclear structure, Phys. Rep. 160 (1988) 235–427, https://doi.org/10.1016/0370-1573(88)90179-2.

[5] C. Ciofi degli Atti, S. Scopetta, E. Pace, G. Salme, Nuclear effects in deep inelastic scattering of polarized electrons off polarized ^{3}He and the neutron spin structure functions, Phys. Rev. C 48 (1993) R968–R972, https://doi.org/10.1103/PhysRevC.48.R968, arXiv:nucl-th/9303016.

[6] W. Melnitchouk, G. Piller, A.W. Thomas, Deep inelastic scattering from polarized deuterons, Phys. Lett. B 346 (1995) 165–171, https://doi.org/10.1016/0370-2693(94)01690-E, arXiv:hep-ph/9501282.

[7] S.A. Kulagin, W. Melnitchouk, G. Piller, W. Weise, Spin dependent nuclear structure functions: General approach with application to the deuteron, Phys. Rev. C 52 (1995) 932–946, https://doi.org/10.1103/PhysRevC.52.932, arXiv:hep-ph/9504377.

[8] G. Piller, W. Melnitchouk, A.W. Thomas, Polarized deep inelastic scattering from nuclei: A relativistic approach, Phys. Rev. C 54 (1996) 894–903, https://doi.org/10.1103/PhysRevC.54.894, arXiv:nucl-th/9605045.

[9] L. Frankfurt, V. Guzey, M. Strikman, The nuclear effects in $g_{1^3\mathrm{He}}$ and the Bjorken sum rule for $A = 3$, Phys. Lett. B 381 (1996) 379–384, https://doi.org/10.1016/0370-2693(96)00625-9, arXiv:hep-ph/9602301.

[10] F.R.P. Bissey, V.A. Guzey, M. Strikman, A.W. Thomas, Complete analysis of spin structure function g_1 of ^{3}He, Phys. Rev. C 65 (2002) 064317, https://doi.org/10.1103/PhysRevC.65.064317, arXiv:hep-ph/0109069.

[11] J.J. Ethier, W. Melnitchouk, Comparative study of nuclear effects in polarized electron scattering from 3He, Phys. Rev. C 88 (5) (2013) 054001, https://doi.org/10.1103/PhysRevC.88.054001, arXiv:1308.3723.

[12] D. Boer, et al., Gluons and the quark sea at high energies: Distributions, polarization, tomography, arXiv:1108.1713.

[13] A. Accardi, et al., Electron ion collider: the next QCD frontier, Eur. Phys. J. A 52 (9) (2016) 268, https://doi.org/10.1140/epja/i2016-16268-9, arXiv:1212.1701.

[14] L.L. Frankfurt, M.I. Strikman, High-energy phenomena, short range nuclear structure and QCD, Phys. Rep. 76 (1981) 215–347, https://doi.org/10.1016/0370-1573(81)90129-0.

[15] M. Sargsian, M. Strikman, Model independent method for determination of the DIS structure of free neutron, Phys. Lett. B 639 (2006) 223–231, https://doi.org/10.1016/j.physletb.2006.05.091, arXiv:hep-ph/0511054.

[16] N. Baillie, et al., Measurement of the neutron F2 structure function via spectator tagging with CLAS, Phys. Rev. Lett. 108 (2012) 142001, https://doi.org/10.1103/PhysRevLett.108.142001, arXiv:1110.2770; Erratum: Phys. Rev. Lett. 108 (2012) 199902, https://doi.org/10.1103/PhysRevLett.108.199902.

[17] S. Tkachenko, et al., Measurement of the structure function of the nearly free neutron using spectator tagging in inelastic ^{2}H(e,e'p)X scattering with CLAS, Phys. Rev. C 89 (2014) 045206, https://doi.org/10.1103/PhysRevC.89.045206, arXiv:1402.2477; Addendum: Phys. Rev. C 90 (2014) 059901, https://doi.org/10.1103/PhysRevC.90.059901.

[18] S. Bueltmann, et al., The structure of the free neutron at large x-Bjorken, Jefferson Lab 12GeV Experiment E12-06-113, Proposal: https://www.jlab.org/exp_prog/proposals/06/PR12-06-113.pdf.

[19] W. Armstrong, et al., Tagged EMC measurements on light nuclei, arXiv:1708.00891.

[20] C. Weiss, et al., Physics potential of polarized light ions with EIC@JLab, Jefferson Lab 2014/2015, Laboratory-directed Research and Development Project, Webpage: https://www.jlab.org/theory/tag/.

[21] W. Cosyn, V. Guzey, D.W. Higinbotham, C. Hyde, S. Kuhn, P. Nadel-Turonski, K. Park, M. Sargsian, M. Strikman, C. Weiss, Neutron spin structure with polarized deuterons and spectator proton tagging at EIC, J. Phys. Conf. Ser. 543 (2014) 012007, https://doi.org/10.1088/1742-6596/543/1/012007, arXiv:1409.5768.

[22] L.L. Frankfurt, M.I. Strikman, High momentum transfer processes with polarized deuterons, Nucl. Phys. A 405 (1983) 557–580, https://doi.org/10.1016/0375-9474(83)90518-3.

[23] W. Cosyn, C. Weiss, in preparation.

[24] M. Strikman, C. Weiss, Electron-deuteron deep-inelastic scattering with spectator nucleon tagging and final-state interactions at intermediate x, Phys. Rev. C 97 (3) (2018) 035209, https://doi.org/10.1103/PhysRevC.97.035209, arXiv:1706.02244.

[25] D.E. Soper, Infinite-momentum helicity states, Phys. Rev. D 5 (1972) 1956–1962, https://doi.org/10.1103/PhysRevD.5.1956.

[26] S.J. Brodsky, H.-C. Pauli, S.S. Pinsky, Quantum chromodynamics and other field theories on the light cone, Phys. Rep. 301 (1998) 299–486, https://doi.org/10.1016/S0370-1573(97)00089-6, arXiv:hep-ph/9705477.

[27] L.A. Kondratyuk, M.I. Strikman, Relativistic correction to the deuteron magnetic moment and angular condition, Nucl. Phys. A 426 (1984) 575–598, https://doi.org/10.1016/0375-9474(84)90165-9.

[28] B.D. Keister, W.N. Polyzou, Relativistic Hamiltonian dynamics in nuclear and particle physics, Adv. Nucl. Phys. 20 (1991) 225–479.

[29] J.R. Cooke, G.A. Miller, Deuteron binding energies and form-factors from light front field theory, Phys. Rev. C 66 (2002) 034002, https://doi.org/10.1103/PhysRevC.66.034002, arXiv:nucl-th/0112037.

[30] R.B. Wiringa, V.G.J. Stoks, R. Schiavilla, An accurate nucleon-nucleon potential with charge independence breaking, Phys. Rev. C 51 (1995) 38–51, https://doi.org/10.1103/PhysRevC.51.38, arXiv:nucl-th/9408016.

[31] F.M. Lev, E. Pace, G. Salme, Electromagnetic and weak current operators for interacting systems within the front form dynamics, Nucl. Phys. A 641 (1998) 229–259, https://doi.org/10.1016/S0375-9474(98)00469-2, arXiv:hep-ph/9807255.

[32] B.D. Keister, Rotational covariance and light front current matrix elements, Phys. Rev. D 49 (1994) 1500–1505, https://doi.org/10.1103/PhysRevD.49.1500, arXiv:hep-ph/9303264.

[33] R.A. Gilman, F. Gross, Electromagnetic structure of the deuteron, J. Phys. G 28 (2002) R37–R116, https://doi.org/10.1088/0954-3899/28/4/201, arXiv:nucl-th/0111015.

[34] B.L.G. Bakker, C.-R. Ji, Frame dependence of spin one angular conditions in light front dynamics, Phys. Rev. D 65 (2002) 073002, https://doi.org/10.1103/PhysRevD.65.073002, arXiv:hep-ph/0109005.

[35] W. Cosyn, M. Sargsian, Nuclear final-state interactions in deep inelastic scattering off the lightest nuclei, Int. J. Mod. Phys. E 26 (09) (2017) 1730004, https://doi.org/10.1142/S0218301317300041, arXiv:1704.06117.